Am J Transl Res 2022;14(6):3854-3863
www.ajtr.org /ISSN:1943-8141/AJTR0142372

Original Article

Binding domain peptide ameliorates alveolar hypercoagulation and fibrinolytic inhibition in mice with lipopolysaccharide-induced acute respiratory distress syndrome Via NF-κB signaling pathway

Yahui Wang[1,2*], Yanqi Wu[1*], Bo Liu[1], Huilin Yang[1], Hong Qian[1], Yumei Cheng[1], Xiang Li[1], Guixia Yang[1], Xinghao Zheng[1], Feng Shen[1]

[1]Department of Intensive Care Unit, Guizhou Medical University Affiliated Hospital, Guiyang 550001, Guizhou, China; [2]Department of Intensive Care Unit, The People's Hospital of Weining County, Weining County 553100, Guizhou, China. [*]Equal contributors.

Received February 15, 2022; Accepted May 7, 2022; Epub June 15, 2022; Published June 30, 2022

Abstract: Background: Alveolar hypercoagulation and fibrinolytic inhibition are shown to be associated with refractory hypoxemia in acute respiratory distress syndrome (ARDS), and the NF-κB pathway is involved in this process. The purpose of this study is to explore the role of NEMO-binding domain peptide (NBDP) in alleviating alveolar hypercoagulation and fibrinolytic inhibition induced by lipopolysaccharide (LPS) in ARDS mice and its related mechanisms. Materials and methods: ARDS was induced by inhalation of LPS (mg/L) in adult male BALB/c mice. Mice were treated with intratracheal inhalation of NBDP or saline aerosol at increased concentrations 30 minutes before LPS administration. Six hours after LPS treatment, bronchoalveolar lavage fluids (BALF) were collected and then all mice were euthanized. In addition, coagulation and fibrinolysis associated factors in lung tissues and BALF were detected, and the activation of NF-κB signaling pathway was observed. Results: NBDP pretreatment dose-dependently inhibited the expression of tissue factor (TF) and plasminogen activator inhibitor (PAI) 1 in lung tissues, reduced the secretions of TF, PAI-1, thrombin-antithrombin (TAT) complex, and promoted activated protein C (APC) secretion in BALF induced by LPS. LPS-induced high expression of pulmonary procollagen peptide type III (PIIIP) was also reduced in a dose-dependent manner under NBDP pretreatment. Western blotting showed that NBDP pretreatment significantly attenuated LPS-induced activation of IKKα/β, Iκα and NF-κB p65. NBDP pretreatment also inhibited the DNA binding activity of p65 induced by LPS. We also noticed that NBDP protected mice against LPS-induced lung injury in a dose-dependent manner. Conclusions: The experimental findings demonstrate that through inhibiting the NF-κB signaling pathway, NBDP dose-dependently ameliorates LPS-induced alveolar hypercoagulation and fibrinolytic inhibition, which is expected to be a new therapeutic target to correct the abnormalities of alveolar coagulation and fibrinolytic pathways in ARDS.

Keywords: Acute respiratory distress syndrome, NEMO-binding domain peptide, NF-κB, alveolar hypercoagulation, fibrinolytic inhibition

Introduction

Respiratory distress syndrome (ARDS), the severe form of acute lung injury (ALI), is one of the most common diseases for admission to the intensive care unit (ICU) and the leading cause of respiratory failure and death in critically ill patients [1]. The complicated pathophysiology of ARDS is one of the important reasons for the treatment difficulty and high mortality of the disease, among which alveolar hypercoagulation and fibrinolytic inhibition are the key factors [2]. Alveolar hypercoagulation and fibrinolysis inhibition results in extensive microthrombus formation in pulmonary vessels, and massive fibrin deposition in the airspace [3, 4], which is closely related to decreased lung compliance, V/Q ratio imbalance and arteriovenous shunting, resulting in refractory hypoxemia in ARDS patients. However, there is currently no satisfactory treatment for the management of hypercoagulation and fibrinolytic inhibition in ARDS due to the complicated mechanisms underlying these pathological processes. Our pre-

vious studies [5, 6] and other published data [7] have confirmed that the nuclear factor kappa B (NF-κB) signaling pathway plays a pivotal role in the pathogenesis of alveolar hypercoagulation and fibrinolytic inhibition.

NF-κB is mainly involved in the regulation of many important physiopathologic processes, such as immunity, inflammation, tumorigenesis and stress responses [8, 9]. Activation of NF-κB results in its translocation from the cytoplasm to the nucleus. Under normal conditions, NF-κB is sequestered in the cytoplasm, where it binds to its inhibitor protein members, including IκBα, IκBβ and IκBγ. The IκB kinase (IKK) complex is required for the activation of NF-κB and consists of three subunits, namely IKKα, IKKβ and IKKγ, of which IKKγ is also known as NEMO. NEMO itself does not have a catalytic domain, but plays a key role in biology as a part of the IKK complex [10, 11]. The NH2-terminus of NEMO binds to a hexapeptide sequence Leu-Asp-Trp-Ser-Trp-Leu at the COOH terminus of IKKα and IKKβ, called the NEMO-binding domain (NBD) [12], which is the basic structure for the crosstalk among IKKα, IKKβ and NEMO, maintaining the biological activity of the IKK complex [13]. Although there are many ways to inhibit NF-κB, such as NF-κB/IKKβ gene knockout or knockdown, NF-κB-specific inhibition, blocking P65 translocation from cytoplasm into the nucleus or preventing P65 from binding to its specific DNA sequence (κB sequence) etc., these methods also inevitably inhibit some basal biological activities of NF-κB [14, 15]. A small molecular NBD peptide (NBDP), however, has been shown not only to selectively inhibit the NF-κB-mediated target gene transcription through targeting the crosstalk between IKK and NEMO [16], but also maintain the important basal activities of NF-κB [17]. In addition, previous studies have demonstrated that NBDP effectively inhibited NF-κB pathway activation [18-21]. Based on these findings, we speculate that NBDP can correct alveolar coagulation and fibrinolysis abnormalities via the NF-κB signaling pathway in ARDS. Thus, the innovation of our study is to investigate the underlying mechanism of NBDP in ARDs. In our study, it is demonstrated that NBDP dose-dependently attenuated lipopolysaccharide (LPS)-induced alveolar hypercoagulation and fibrinolytic inhibition by inactivating the NF-κB signaling pathway in mice, and NBDP is expected to be a new significant target in the treatment of ARDS.

Materials and methods

Experimental animals

BALB/c male mice, aged 6-8 weeks and weighing 20-25 g, were purchased from the Animal Center of Guizhou Medical University. All mice were fed a normal standard diet in a controlled environment (temperature 22 ± 1°C) with a 12 hour light/dark cycle and controlled humidity. The mice were given 7 days to acclimatize to the environment prior to the experiment. The study was approved by the Animal Ethics Committee of Guizhou Medical University and was conducted in accordance with guidelines of the Chinese Laboratory Animal Management Regulations.

Animal model establishment

A mouse model of ARDS was established by aerosol inhalation of LPS. Seventy-two mice were randomly divided into the following six groups: Control, Model, N-NBD, L-NBD, M-NBD and H-NBD, with 12 in each group. The mice in Model, N-NBD, L-NBD, M-NBD and H-NBD received 50 μl of LPS (4 mg/ml, Sigma-Aldrich) while those in the control group received the same volume of saline inhalation. Thirty minutes before LPS administration, mice in L-NBD, M-NBD and H-NBD groups inhaled 50 μl of NBDP (MERCK) with the concentration of 120 μg/ml, 240 μg/ml and 360 μg/ml, respectively. The N-NBD group served as a negative control and received a non-functional NBDP analogue (50 μl, MERCK) at a concentration of 240 μg/ml. Six hours after LPS or saline inhalation, all mice were euthanized via cervical dislocation and exsanguination under anesthesia with pentobarbital sodium (50 mg/kg). Bronchoalveolar lavage fluid (BALF) samples were collected for the detection of coagulation-related factors. Left lung tissues of mice were collected for histopathological and immunohistochemical analysis while right lungs were immediately frozen in liquid nitrogen and stored at -80°C for enzyme-linked immunosorbent assay (ELISA) and western blot (WB) analysis.

Real-time quantitative PCR (RT-qPCR)

RT-qPCR was performed to detect tissue factor (TF) and plasminogen activator inhibitor-1 (PAI-1) gene expression. The concentration of total RNA was detected by using a NanoDrop-2000 spectrophotometer (NanoDrop Technologies,

Table 1. Gene sequences of TF, PAI-1

Gene	Sequences
TF	5-AGA CGG AGA CCA ACT TGT GAT-3
	5-CTG CTG AAT TAC TGG CTG TCC-3
PAI-1	5-CTG CAA AAG GTC AGG ATC GAG-3
	5-CAT CAC TTG GCC CAT GAA GAG-3
β-actin	5-CAC CCG CGA GTA CAA CCT TC-3
	5-CCA ATA CCC ACC ATC ACA CC-3

Germany) and the A260/A280 ratio of the extracted RNA was controlled between 1.8 to 2.0. Primers were designed based on the TF and PAI-1 gene sequences supplied by the NCBI gene database. The primers were synthesized by Guangzhou Aiji Biotechnology Co., Ltd. (**Table 1**). PCR amplification was performed using cDNA as the template. The reaction system was set as follows: SYBR Green Mix 10 μl, forward primer and reverse primer 0.8 μl each, cDNA template 0.8 μl, and ddH20 7.6 μl into a system containing 20 μl reagents. The dissolution and amplification curves of genes were recorded following gene amplification. The relative expression levels of target genes were calculated using the $2^{-\Delta\Delta Ct}$ method.

Western blot

Cytoplasmic proteins were extracted using the Cell Solute Extraction Kit according to the manufacturer's instructions (Solebao Technology Co., Ltd, Beijing, China). Briefly, the concentration of protein was measured using a bicinchoninic acid (BCA) assay kit (Thermo Scientific, Waltham, MA). An equal amount of protein from each sample was resolved in 12% Tris-glycine sodium dodecyl sulfate (SDS) polyacrylamide gel. The protein bands were blotted onto a nitrocellulose membrane. After incubating for 2 hours in blocking solution, the membrane was incubated with p-P65 (ab76302, Abcam, UK), p-IKKα/β (ab194528, Abcam, UK), p-IκBα (#2859S, Cell Signaling Technology, USA), PAI-1 (ab222754, Abcam, UK), and TF (ab228968, Abcam, UK) antibodies (all diluted at 1:1000) for 24 hours. Then the secondary antibody horseradish peroxidase-conjugated goat anti-rabbit immunoglobulin (1:2000 dilution, #7074S, Cell Signaling Technology, USA) was added and incubated for 2 hours at 37°C. The target protein bands were visualized using an enhanced chemiluminescence detection system (Millipore, MA, USA). Relative band densities were quantified by Image J software.

ELISA assay

The collected BALF was centrifuged at 4500 rpm for 10 minutes at 4°C, and the resulting supernatant was collected and stored at -80°C for testing. TF, PAI-1 and activated protein C (APC) levels were determined using ELISA kits (Huamei Bio-company, Wuhan, China) according to the manufacturer's instructions.

Histopathology

The lung tissues were fixed with 4% paraformaldehyde for 24 hours, followed by dehydration, paraffin-embedding and slicing (4 μm). Then the slices were stained with hematoxylin-eosin (H&E). The scores of lung injury were blindly evaluated by pathologists, as described previously [22]. Each histological change was scored (lung injury score, LIS) from 0 to 3 according to the lesion range, including alveolar wall thickening, edema, inflammatory cell infiltration, hemorrhage and cellulose deposition (0: normal; 1: injury ≤ 25% of the field; 2: injury within 25%-50% of the field; 3: injury ≥ 50% of the field).

NF-κB p65 DNA binding activity

The DNA binding activity of NF-κB p65 in the right upper lung tissues was detected using the Universal EZ-TFA Transcription Factor Chemiluminescence Kit (Millipore, Germany) according to the manufacturer's instructions. The nuclear extract of lung tissues was added to a plate containing biotinylated oligonucleotide which had NF-κB binding site. After incubating for 1 hour at room temperature, the plate was washed and incubated with rabbit anti-NF-κB p65 (1:1000 dilution) for 1 hour. After washing the plate, an anti-rabbit horseradish peroxidase-conjugated antibody (1:500 dilution) was added and incubated for 30 minutes. This was followed by the addition of the chemiluminescent substrate solution for 5 minutes of incubation. The sample OD value was read by a microplate reader at 1-s integration time.

Immunohistochemistry (IHC)

After dehydration of paraffin sections in ethanol series, the antigens were retrieved using a citrate buffer. The nonspecific binding site was blocked by 3% BSA. The sections were incubated with rabbit anti-mouse P65 (1:600, #6956S, Cell Signaling Technology, USA) and type III col-

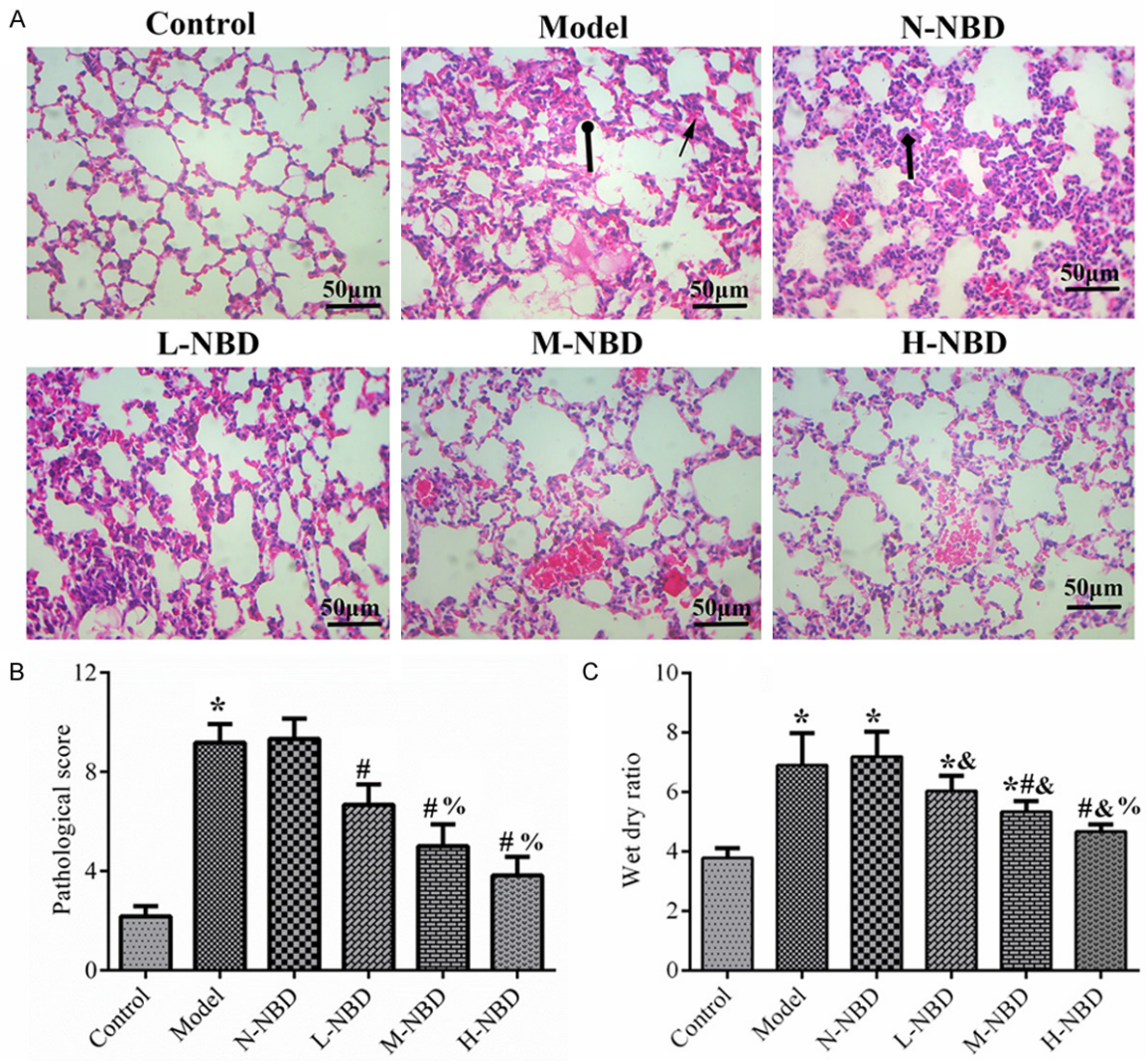

Figure 1. Pathological changes in the lung tissues. A: Lung sections were stained with hematoxylin and eosin 6 hours after LPS administration. LPS destroyed the lung tissues, resulting in hemorrhage (↗), inflammatory cell infiltration (↑), alveolar wall thickening (↑) and so on, which were all attenuated by NBDP pretreatment; B: NBDP pretreatment significantly alleviated these pathological changes; C: NBDP pretreatment significantly alleviated pulmonary edema. Data were expressed as mean ± SD (n=6). *P<0.05 compared with Control. #P<0.05 compared with Model. &P<0.05 compared with N-NBD. %P<0.05 compared with L-NBD.

lagen (1:200, ab7778, Abcam, UK) antibodies at 4°C overnight, followed by washing and incubating with corresponding HRP-labeled secondary antibodies (1:1000, ab6721, Abcam, UK) for 1 hour at room temperature. The expression levels of antigens were visualized using peroxidase activity developed by DAB staining solution and observed at a magnification of 400X.

Statistical analysis

Statistical analyses were performed with SPSS. Data was expressed as mean ± SD. Statistical differences were determined by one-way analysis of variance (ANOVA) and the Student-Newman-Keuls (SNK) method, with the significance level set as $P<0.05$.

Results

NBDP improved pulmonary pathological changes induced by LPS inhalation in mice

H&E staining and histopathological analysis were performed to assess the pathological changes of pulmonary tissues and the degree

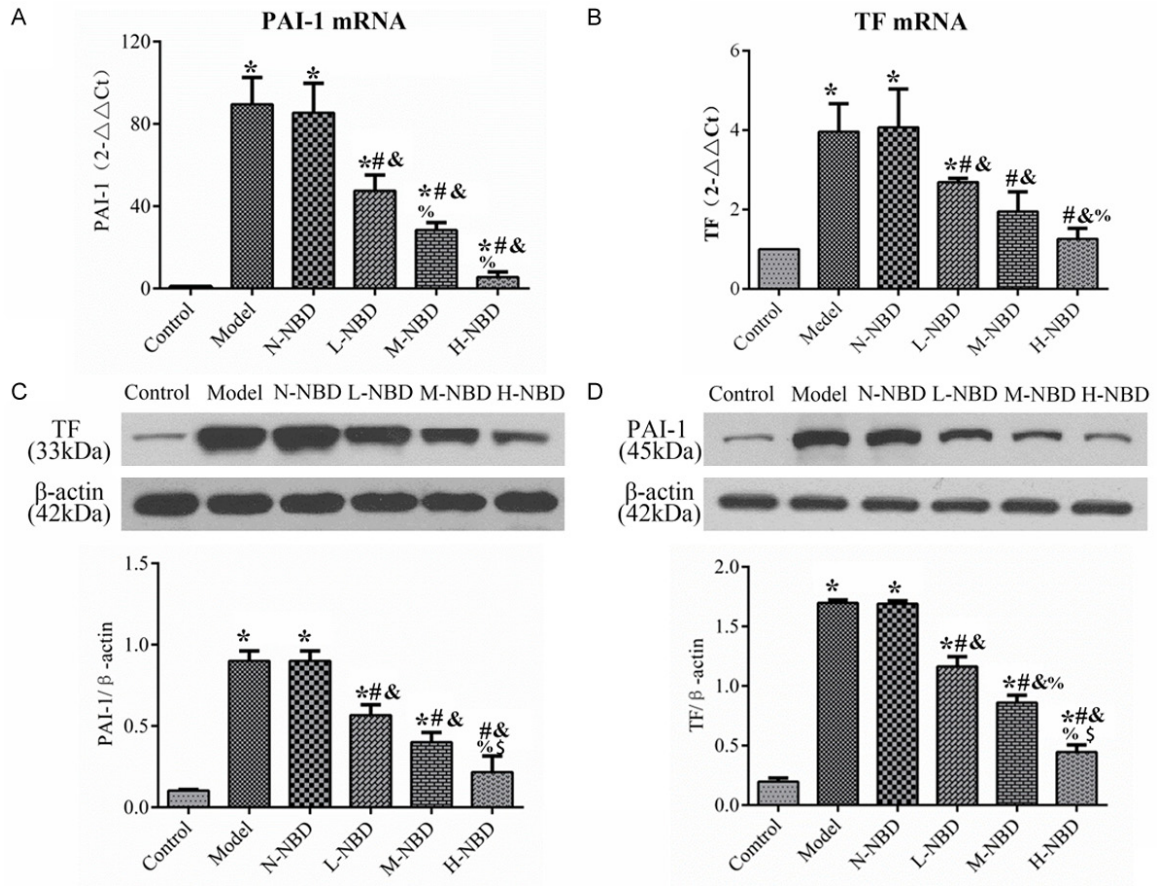

Figure 2. Changes of TF and PAI-1 expression in pulmonary tissue 6 hours after LPS inhalation with or without NBDP pretreatment. A: RT-qPCR was performed to detect TF mRNA expression in lung tissues; B: RT-qPCR was performed to detect PAI-1 mRNA expression in lung tissues; C: Western blotting was performed to detect TF protein expression in lung tissues; D: Western blotting was performed to detect PAI-1 protein expression in lung tissues. Each bar represents the mean ± SD of 6 mice. *P<0.05 compared with Control. #P<0.05 compared with Model. &P<0.05 compared with N-NBD. %P<0.05 compared with L-NBD. $P<0.05 compared with M-NBD.

of lung injury. It was found that LPS induced excessive edema, obvious inflammatory cell infiltration, alveolar collapse, alveolar wall thickening, and severe hemorrhage, which were all dose-dependently inhibited by NBDP. The LPS-induced high W/D ratio and LIS were also significantly reduced by NBDP treatment (**Figure 1**).

NBDP attenuated mRNA and protein levels of TF and PAI-1 in LPS-induced ARDS mice

In order to evaluate the coagulation and fibrinolytic status of LPS-induced lung tissues, TF and PAI-1 were measured by RT-qPCR and WB. The results showed that LPS stimulated high mRNA and protein expression of TF and PAI-1 in lung tissues, which were effectively attenuated by NBDP pretreatment (**Figure 2**).

NBDP inhibited LPS-induced secretions of TF, PAI-1, and thrombin-antithrombin (TAT) in lung tissue and promoted APC production

The levels of TF, PAI-1, TAT and APC in BALF were determined by ELISA to evaluate the degree of alveolar hypercoagulation and fibrinolytic inhibition. LPS stimulation for 6 hours resulted in obvious increases in TF, PAI-1 and TAT levels and a decrease in APC level in BALF, all of which were reversed by NBDP in a dose-dependent manner (**Figure 3**).

NBDP alleviated LPS-induced PIIIP deposition in mouse lung tissue

The levels of PIIIP in mouse lung tissue was detected using immunohistochemistry to evaluate the effect of LPS on fibrinolystic inhibi-

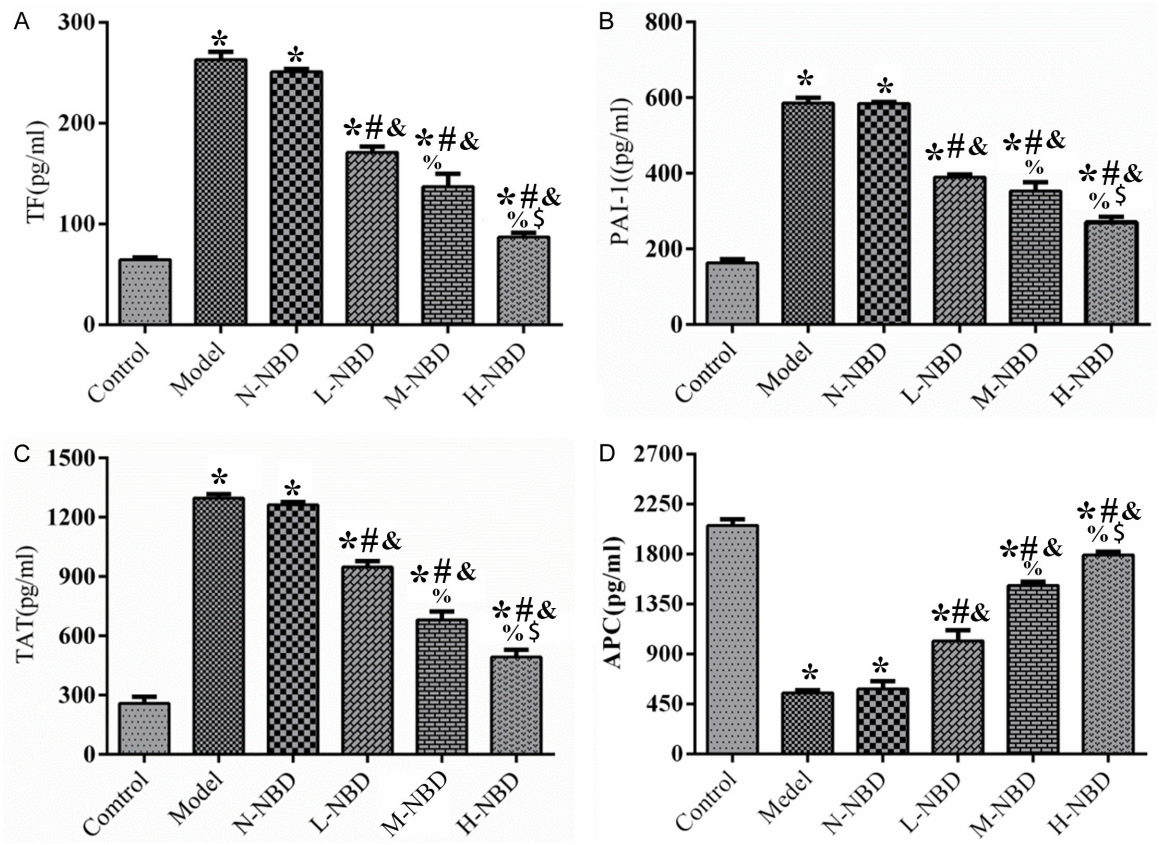

Figure 3. NBDP significantly inhibited TF, PAI-1, and TAT, and promoted APC secretions in LPS-induced lung tissues. A: ELISA detection of the changes of TF following LPS induction with or without NBDP. B: ELISA detection of the changes of PAI-1 following LPS induction with or without NBDP; C: ELISA detection of the changes of TAT following LPS induction with or without NBDP; D: ELISA detection of the changes of APC secretions following LPS induction with or without NBDP; Values were presented as mean ± SD. *P<0.05 compared with Control. $^{\#}$P<0.05 compared with Model. $^{\&}$P<0.05 compared with N-NBD. $^{\%}$P<0.05 compared with L-NBD. $^{\$}$P<0.05 compared with M-NBD.

tion. The results demonstrated that LPS induced a large amount of PIIIP in pulmonary tissues. After pretreatment with NBD, LPS-induced PIIIP deposition was significantly reduced in a dose-dependent manner (**Figure 4**).

NBDP inhibited LPS-induced NF-κB activation

To assess the effects of NBDP on NF-κB signaling pathway, WT was performed to detect the phosphorylation of IKKα/β, IκBα and P65 after LPS stimulation. Significant increases were observed in IKKα/β (p-IKKα/β), p-IκBα and p-P65 phosphorylation levels in LPS-induced lung tissues, which were weakened by NBDP pretreatment (**Figure 5**).

NBDP decreased P65 DNA binding activity initiated by LPS stimulation

NF-κB p65 DNA binding activity is related to P65 translocation from cytoplasm to nucleus. Our data showed that NF-κB p65 DNA binding activity was significantly increased after LPS stimulation, which was dose-dependently decreased by NBDP (**Figure 6**).

Discussion

In this study, an ARDS mouse model simulating the pathogenesis of ARDS was successfully constructed [22]. Meanwhile, we found that NBDP effectively ameliorated LPS-induced hypercoagulation and fibrinolysis inhibition in lung tissues and the airspace, which was consistent with the research of Huang et al. [23]. These findings suggested that NBD has potential as a therapeutic target in the treatment of acute inflammatory diseases, including ALI, ARDS, and infectious diseases.

TF is a potent procoagulant that initiates the extrinsic coagulation cascade mainly through interacting with Factor VII in the presence of

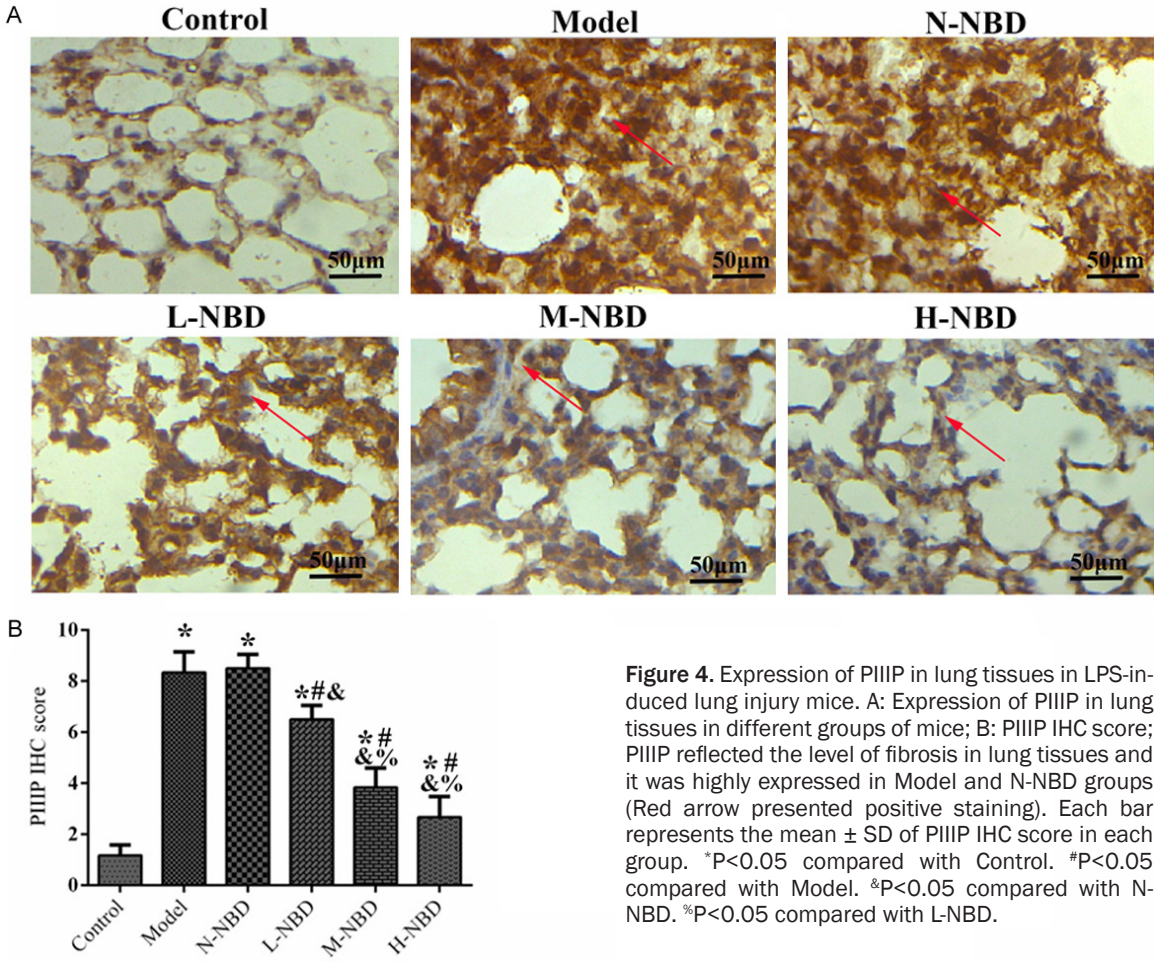

Figure 4. Expression of PIIIP in lung tissues in LPS-induced lung injury mice. A: Expression of PIIIP in lung tissues in different groups of mice; B: PIIIP IHC score; PIIIP reflected the level of fibrosis in lung tissues and it was highly expressed in Model and N-NBD groups (Red arrow presented positive staining). Each bar represents the mean ± SD of PIIIP IHC score in each group. *P<0.05 compared with Control. #P<0.05 compared with Model. &P<0.05 compared with N-NBD. %P<0.05 compared with L-NBD.

calcium, resulting in activation of Factor X [24, 25]. PAI-1 is a major physiological inhibitor of the fibrinolytic system that can also regulate thrombosis [26]. PAI-1 binds to and inhibits tissue and urokinase-type plasminogen activators (tPA and uPA), thereby reducing plasmin production and fibrin clot lysis [27]. The results of our study showed that the mRNA and protein expression of both TF and PAI-1 were highly expressed in pulmonary tissue under LPS stimulation, indicating the presence of procoagulation and fibrinolytic defects in lung tissues [28].

TAT is a complex of thrombin and antithrombin that directly reflects the generation of thrombin, with an increase in TAT suggesting a state of procoagulant activity [29]. APC is a protein synthesized by the liver and exerts anticoagulant activity by hydrolyzing blood coagulation factors Va and VIIIa [30]. Our experimental data showed that in BALF, the concentrations of TF, PAI-1, and TAT were all significantly increased, while APC concentration was statistically decreased, indicating hypercoagulation and fibrinolytic inhibition in the airspace in LPS-induced ARDS [31].

PIIIP is mainly synthesized and secreted by fibroblasts and transformed in myofibroblasts. In addition, PIIIP is the main component of the extracellular matrix (ECM), and the excessive accumulation of PIIIP suggests pulmonary fibrous deposition [32]. High expression of pulmonary PIIIP under LPS treatment in our study indicated an increase in fibrous tissue in the lung due to fibrinolytic inhibition.

NBDP is a protein peptide that has been shown to inhibit the activation of the classical NF-κB signaling pathway by interfering with the NEMO-IKKα/IKKβ interaction [33]. Our data demonstrated that NBDP pretreatment significantly inhibited LPS-induced NF-κB pathway activation, manifested as decreased levels of p-IKKα/β, p-Iκα and p-P65, and decreased P65

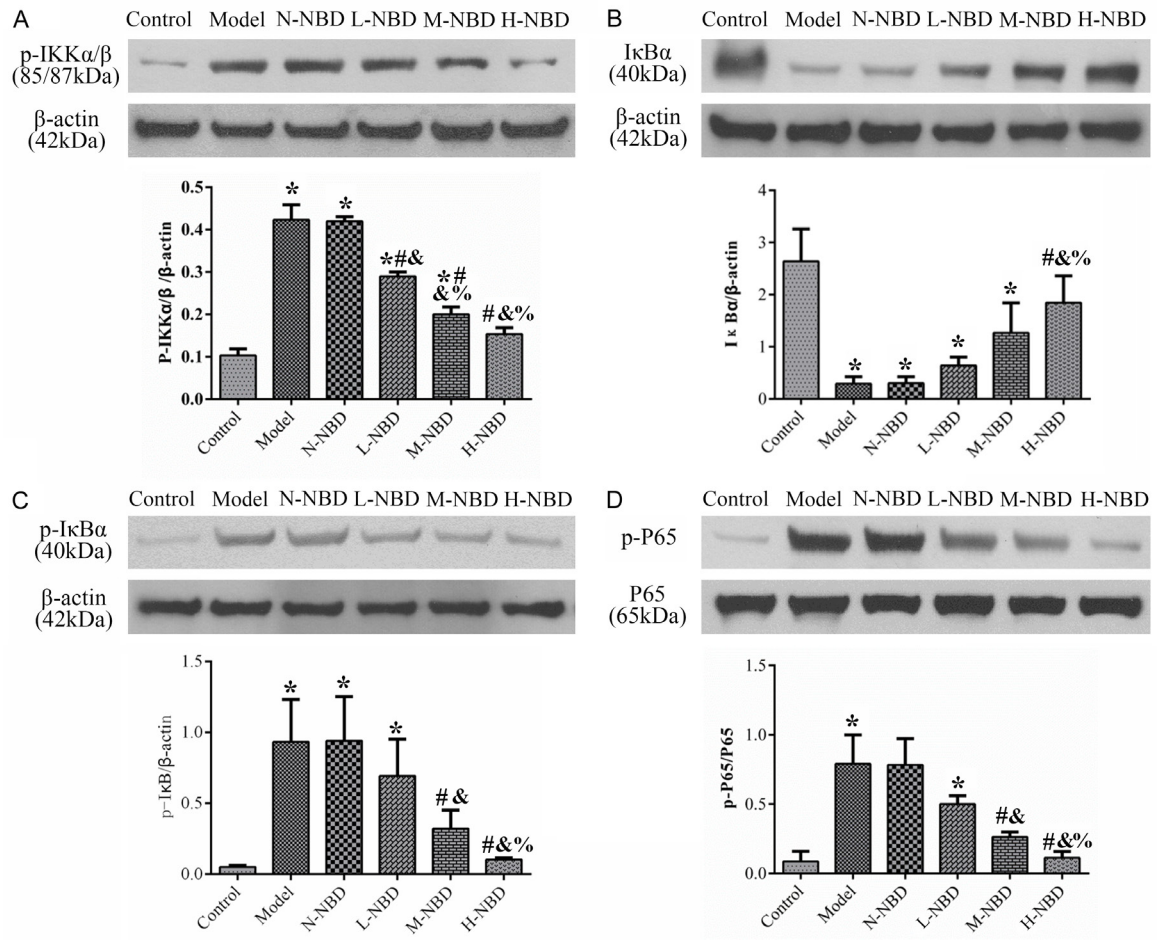

Figure 5. NBDP inhibited LPS-induced activation of NF-κB signal pathway. A: Western blotting results of p-IKKα/β; B: Western blotting results of IκBα; C: Western blotting results of p-IκBα; D: Western blotting results of p-P65. The quantitative data were presented as mean ± SD of 6 mice. *P<0.05 compared with Control. #P<0.05 compared with Model. &P<0.05 compared with N-NBD. %P<0.05 compared with L-NBD.

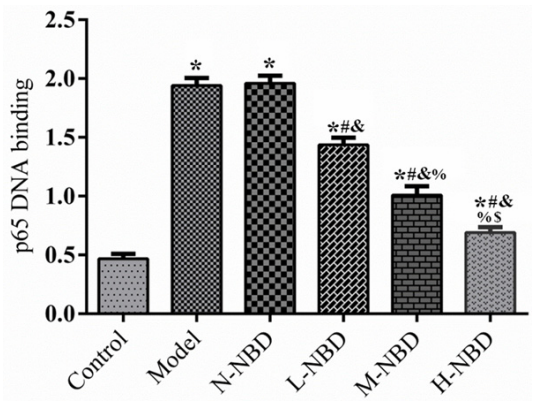

Figure 6. NBDP decreased the enhanced p65 DNA binding activity induced by LPS inhalation. DNA binding activity of NF-κB p65 was examined by a TransAM p65 transcription factor ELISA kit. Each bar represents the mean ± SD of 6 mice. *P<0.05 compared with Control. #P<0.05 compared with Model. &P<0.05 compared with N-NBD. %P<0.05 compared with L-NBD. $P<0.05 compared with M-NBD.

NDA binding activity. In addition, NBDP effectively suppressed TF and PAI-1 expression in pulmonary tissue, and reduced TF, PAI-1 and TAT secretions in BALF while promoting APC production in BALF. Therefore, NBDP can correct alveolar hypercoagulation and fibrinolytic inhibition induced by LPS via inactivating the NF-κB pathway. Interestingly, we found that the higher the dose of NBDP, the more obvious the effects of NBDP on coagulation and fibrinolysis associated factors and NF-κB inactivation, indicating a dose-dependent manner.

Unlike other inhibitors or methods, such as gene knockdown, knockout or specific inhibitor, NBDP has been shown to selectively inhibit NF-κB-mediated target gene transcription while maintaining the important basal activities of NF-κB [16, 17], allowing it to be a new potential therapeutic target in ARDS treatment.

In this study, a negative control group with non-functional NBDP analogue (50 μl, MERCK) was set up to eliminate the effect of NBDP itself on the experimental results. Overall, however, there are still some limitations to be addressed. First, the lack of arterial blood gas analysis made the diagnosis of ARDS insufficient. Second, although we pretreated LPS induced mice with different doses of NBDP, the optimal dose to weaken hypercoagulability and fibrinolysis inhibition and the optimal timing of administration remain to be clarified. Nevertheless, the findings of our study showed that NBDP dose-dependently ameliorates LPS-induced alveolar hypercoagulation and fibrinolytic inhibition through inhibiting the NF-κB signaling pathway, suggesting that NBDP is a promising therapeutic choice for the treatment of ARDS and deserves further exploration.

Conclusions

NBDP dose-dependently ameliorates alveolar hypercoagulation and fibrinolysis inhibition via the NF-κB signaling pathway, which is expected to be a new effective therapeutic target for ARDS.

Acknowledgements

We thank Mr. Yi FANG and Professor Xu LIU, who greatly assisted our experiments. This study was supported by a grant from Guizhou Science and Technology Plan Project ([2019]1261), and also was supported by the National Natural Science Foundation of China [82160365].

Disclosure of conflict of interest

None.

Abbreviations

NBDP, NEMO-Binding Domain Peptide; ARDS, Acute respiratory distress syndrome; ALI, Acute lung injury; BALF, Bronchoalveolar lavage fluids; TF, Tissue factor; PAI-1, Plasminogen activator inhibitor 1; TAT, Thrombin-antithrombin complex; APC, Activated protein C; PIIIP, Procollagen peptide type III; WB, Western blotting; IHC, Immunohistochemistry; tPA, Tissue plasminogen activator; uPA, Urokinase-type plasminogen activators.

Address correspondence to: Feng Shen, Department of Intensive Care Unit, Guizhou Medical University Affiliated Hospital, No. 28, Guiyi Street, Yunyan District, Guiyang 550001, Guizhou, China. Tel: +86-135-1199-9117; E-mail: gyyxydrshen@hotmail.com

References

[1] Bellani G, Laffey JG, Pham T, Fan E, Brochard L, Esteban A, Gattinoni L, Van Haren F, Larsson A and McAuley DF. Epidemiology, patterns of care, and mortality for patients with acute respiratory distress syndrome in intensive care units in 50 countries. JAMA 2016; 315: 788-800.

[2] de Luis Cabezón N, Sánchez Castro I, Bengoetxea Uriarte UX, Rodrigo Casanova MP, García Peña JM and Aguilera Celorrio L. Acute respiratory distress syndrome: a review of the Berlin definition. Rev Esp Anestesiol Reanim 2014; 61: 319-327.

[3] Mokra D and Kosutova P. Biomarkers in acute lung injury. Respir Physiol Neurobiol 2015; 209: 52-58.

[4] Ware LB and Matthay MA. The acute respiratory distress syndrome. N Engl J Med 2000; 342: 1334-1349.

[5] Liu B, Wu Y, Wang Y, Cheng Y, Yao L, Liu Y, Qian H, Yang H and Shen F. NF-κB p65 Knock-down inhibits TF, PAI-1 and promotes activated protein C production in lipopolysaccharide-stimulated alveolar epithelial cells type II. Exp Lung Res 2018; 44: 241-251.

[6] Liu B, Wang Y, Wu Y, Cheng Y, Qian H, Yang H and Shen F. IKKβ regulates the expression of coagulation and fibrinolysis factors through the NF-κB canonical pathway in LPS-stimulated alveolar epithelial cells type II. Exp Ther Med 2019; 18: 2859-2866.

[7] Ding R, Zhao D, Li X, Liu B and Ma X. Rho-kinase inhibitor treatment prevents pulmonary inflammation and coagulation in lipopolysaccharide-induced lung injury. Thromb Res 2017; 150: 59-64.

[8] Bonizzi G and Karin M. The two NF-κB activation pathways and their role in innate and adaptive immunity. Trends Immunol 2004; 25: 280-288.

[9] Hayden MS and Ghosh S. Signaling to NF-κB. Genes Dev 2004; 18: 2195-2224.

[10] Zheng C, Yin Q and Wu H. Structural studies of NF-κB signaling. Cell Res 2011; 21: 183-195.

[11] Israël A. The IKK complex, a central regulator of NF-κB activation. Cold Spring Harb Perspect Biol 2010; 2: a000158.

[12] May MJ, Marienfeld RB and Ghosh S. Characterization of the IκB-kinase NEMO binding domain. J Biol Chem 2002; 277: 45992-46000.

[13] Kensche T, Tokunaga F, Ikeda F, Goto E, Iwai K and Dikic I. Analysis of nuclear factor-κB (NF-κB) essential modulator (NEMO) binding to linear and lysine-linked ubiquitin chains and its role in the activation of NF-κB. J Biol Chem 2012; 287: 23626-23634.
[14] Ward C, Schlingmann B, Stecenko AA, Guidot DM and Koval M. NF-κB inhibitors impair lung epithelial tight junctions in the absence of inflammation. Tissue Barriers 2015; 3: e982424.
[15] Zhang Q, Lenardo MJ and Baltimore D. 30 years of NF-κB: a blossoming of relevance to human pathobiology. Cell 2017; 168: 37-57.
[16] May MJ, D'Acquisto F, Madge LA, Glockner J, Pober JS and Ghosh S. Selective inhibition of NF-κB activation by a peptide that blocks the interaction of NEMO with the IκB kinase complex. Science 2000; 289: 1550-1554.
[17] Khaja K and Robbins P. Comparison of functional protein transduction domains using the NEMO binding domain peptide. Pharmaceuticals 2010; 3: 110-124.
[18] venningsson A, Falk E, Celius EG, Fuchs S, Schreiber K, Berkö S, Sun J and Penner IK; Tynergy Trial Investigators. Natalizumab treatment reduces fatigue in multiple sclerosis. Results from the TYNERGY trial; a study in the real life setting. PLoS One 2013; 8: e58643.
[19] Huang J, Li L, Yuan W, Zheng L, Guo Z and Huang W. NEMO-binding domain peptide attenuates lipopolysaccharide-induced acute lung injury by inhibiting the NF-κB signaling pathway. Mediators Inflamm 2016; 2016: 7349603.
[20] Wu Y, Wang Y, Liu B, Cheng Y, Qian H, Yang H, Li X, Yang G, Zheng X and Shen F. SN50 attenuates alveolar hypercoagulation and fibrinolysis inhibition in acute respiratory distress syndrome mice through inhibiting NF-κB p65 translocation. Respir Res 2020; 21: 1-10.
[21] Zhuang Z, Li H, Lee H, Aguilar M, Gocho T, Ju H, Iida T, Ling J, Fu J and Wu M. NEMO peptide inhibits the growth of pancreatic ductal adenocarcinoma by blocking NF-κB activation. Cancer Lett 2017; 411: 44-56.
[22] Zilberman-Rudenko J, Shawver LM, Wessel AW, Luo Y, Pelletier M, Tsai WL, Lee Y, Vonortas S, Cheng L and Ashwell JD. Recruitment of A20 by the C-terminal domain of NEMO suppresses NF-κB activation and autoinflammatory disease. Proc Natl Acad Sci U S A 2016; 113: 1612-1617.
[23] Schuster DP. ARDS: clinical lessons from the oleic acid model of acute lung injury. Am J Respir Crit Care Med 1994; 149: 245-260.
[24] Bastarache JA, Wang L, Geiser T, Wang Z, Albertine KH, Matthay MA and Ware LB. The alveolar epithelium can initiate the extrinsic coagulation cascade through expression of tissue factor. Thorax 2007; 62: 608-616.
[25] Ahmad S, Ahmad A, Rancourt RC, Neeves KB, Loader JE, Hendry-Hofer T, Di Paola J, Reynolds SD and White CW. Tissue factor signals airway epithelial basal cell survival via coagulation and protease-activated receptor isoforms 1 and 2. Am J Respir Cell Mol Biol 2013; 48: 94-104.
[26] Poole LG, Massey VL, Siow DL, Torres-Gonzáles E, Warner NL, Luyendyk JP, Ritzenthaler JD, Roman J and Arteel GE. Plasminogen activator inhibitor-1 is critical in alcohol-enhanced acute lung injury in mice. Am J Respir Cell Mol Biol 2017; 57: 315-323.
[27] Damare J, Brandal S and Fortenberry YM. Inhibition of PAI-1 antiproteolytic activity against tPA by RNA aptamers. Nucleic Acid Ther 2014; 24: 239-249.
[28] Idell S. Coagulation, fibrinolysis, and fibrin deposition in acute lung injury. Crit Care Med 2003; 31 Suppl: S213-S220.
[29] Lee SY, Niikura T, Iwakura T, Sakai Y, Kuroda R and Kurosaka M. Thrombin-antithrombin III complex tests: a useful screening tool for postoperative venous thromboembolism in lower limb and pelvic fractures. J Orthop Surg 2017; 25: 0170840616684501.
[30] Christiaans SC, Wagener BM, Esmon CT and Pittet JF. Protein C and acute inflammation: a clinical and biological perspective. Am J Physiol Lung Cell Mol Physio 2013; 305: L455-L466.
[31] Alcorn J and Chojkier M. Procollagen III peptide (PIIIP): can it reflect hepatic fibrosis? Hepatology 1987; 7: 981-983.
[32] Camprubí-Rimblas M, Tantinyà N, Bringué J, Guillamat-Prats R and Artigas A. Anticoagulant therapy in acute respiratory distress syndrome. Ann Transl Med 2018; 6: 36.
[33] Dai S, Hirayama T, Abbas S and Abu-Amer Y. The IκB kinase (IKK) inhibitor, NEMO-binding domain peptide, blocks osteoclastogenesis and bone erosion in inflammatory arthritis. J Biol Chem 2004; 279: 37219-37222.